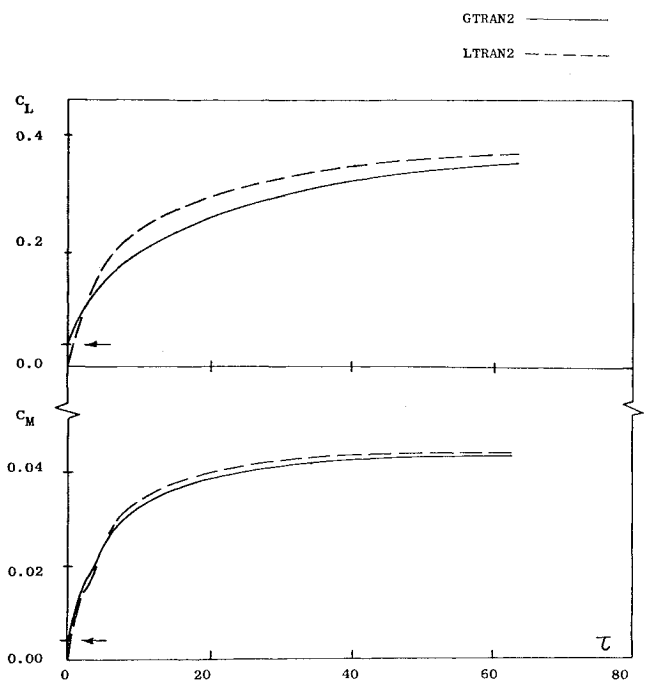

Fig. 3 Impulsive change in angle of attack.

Results obtained using both larger and smaller $\Delta\tau$ increments indicated that these choices adequately insured numerical accuracy. A nonuniform computational mesh consisting of 113 ξ and 97 η points, with 48 points lying over the chord was used. Minimum grid spacings were $\Delta\xi = 0.0025$ and $\Delta\eta = 0.01$ with the computation box defined by $200.0 > |\xi|$ and $397.8 > |\eta|$.

Oscillation cases were time integrated over four periods for $k = 0.05$, 0.5, and 5.0. Figure 1 compares low- and general-frequency results for a $\alpha = \pm 1$ deg airfoil pitching oscillation about the midchord for the unsteady lift and pitching moment coefficients (the moment is taken about the pitch point). At $k = 0.05$, the results are similar except that peak C_L's and C_M's are slightly overpredicted by the low-frequency approximation. With $k = 0.5$, the results appear to agree in phase, but amplitudes differ by about 30%. At $k = 5.0$, a phase difference of about 45 deg is observed in addition to differences in predicted amplitude levels. As k increases, there is a reduction in lift due to a decrease in the shock excursion; the moment, however, remains high because of the shock traversing the pitch point. Physical considerations suggest that shock excursion amplitudes decrease with increasing k. This is confirmed numerically in both models; decay rates in LTRAN2, however, far exceed those observed in GTRAN2. Figure 2 compares results for a $\alpha = \pm 1$ deg trailing edge flap oscillation about $\xi = 0.75$. Results for $k = 0.05$ are similar to those for airfoil oscillation. For $k = 0.5$, however, the low-frequency result overpredicts the moment, unlike the airfoil oscillation case. The lift and moment are substantially lower for the flap oscillation than for the airfoil oscillation case due to the presence of a shock lying upstream of the unsteady disturbance. Finally, we considered impulsive changes in angle of attack from 0-1 deg. The time response to such a step change is often used in modeling gusts or for performing aeroelastic calculations by the indicial method.[3] Time histories for the lift and moment taken about midchord appear in Fig. 3 where $k = 1.0$. For small time, the general-frequency solution shows an abrupt increase in both C_L and C_M. This agrees qualitatively with solutions of the Euler equations[4]; however, this is not obtained in the low-frequency approximation. Apparently the high-frequency components of the unsteady disturbance are critical during this transient period. Both solutions however tend to the same asymptote.

Concluding Remarks

An ADI scheme for general unsteady motions is developed requiring only simple modifications to LTRAN2. Computed results for three different problems indicate the importance of the unsteady terms in high-frequency and gustlike motions. For the cases considered, good agreement was found for low reduced frequencies. For these problems, LTRAN2 is more cost efficient.

Acknowledgment

The authors are grateful to W. F. Ballhaus and P. M. Goorjian for making LTRAN2 available for their use and to H. Yoshihara for some helpful discussions.

References

[1] Ballhaus, W. F. and Goorjian, P. M., "Implicit Finite-Difference Computations of Unsteady Transonic Flows About Airfoils," *AIAA Journal*, Vol. 15, Dec. 1977, pp. 1728-1735.

[2] Ballhaus, W. F. and Steger, J. L., "Implicit Approximate Factorization Schemes for the Low-Frequency Transonic Equation," NASA TMX-73,082, Nov. 1975.

[3] Ballhaus, W. F. and Goorjian, P. M., "Calculation of Unsteady Transonic Flows by the Indicial Method," *AIAA Journal*, Vol. 16, Feb. 1978, pp. 117-124.

[4] Magnus, R. J., "Calculation of Some Unsteady Transonic Flows About the NACA 64A006 and 64A010 Airfoils," AFFDL-TR-77-46, July 1977.

Transport Physics and Mathematical Characteristics

Gustave Hokenson*
Biphase Energy Systems, Santa Monica, Calif.

FLUID dynamic computations of continuum flows are usually based on the hypothesis that the molecular dynamics are in equilibrium with the local macroscopic flowfield state.[1,2] Within this framework, determination of the analytical form of the stress tensor and transport coefficients (for sufficiently dilute media) traditionally relies on Chapman-Enskog solutions to the Boltzmann equation.[3] These relate the transport coefficients to local thermodynamic variables and provide linear algebraic relationships between transport fluxes and the spatial gradients of relevant macroscopic flowfield variables.[4] Higher order transport effects[5-7] that modify linear algebraic theory have not received much attention in continuum flows, inasmuch as the required flowfield time constant becomes significantly smaller than that which is generally established. However, various solutions of Boltzmann's equation in rarefied gases[6] inherently include nonequilibrium effects that are confirmed experimentally.

Results of computations carried out utilizing gradient transport modeling have been verified for a wide range of conditions and are generally accepted. There are, however, mathematical consequences peculiar to the use of these diffusive models. Of primary importance are the infinite "signal" propagation speed and the associated asymptotic nature of solutions to the resultant conservation relations.

Received Nov. 2, 1978; revision received Feb. 20, 1979.

Index categories: Supersonic and Hypersonic Flow, Boundary Layers and Convective Heat Transfer—Laminar, Rarefied Flows.

*Manager of Research, Subsidiary of Research-Cottrell. Member AIAA.

The time-dependent Navier-Stokes equations or the steady boundary-layer equations form a parabolic set of relationships which most clearly illustrate the solution anomalies introduced by the equilibrium assumption.

It is not anticipated that inclusion of nonequilibrium effects encountered in higher order transport theory would often result in significant differences from the flowfields computed with equilibrium, gradient transport models. However, it is important to ascertain whether theoretically based relaxation effects[6] uniquely account for the nonasymptotic nature of real flows. In this regard, a first-order relaxation model for the stress tensor (τ_{ij}) is adopted in the following form:

$$\epsilon \frac{D\tau_{ij}}{Dt} + \tau_{ij} = \tau^*_{ij} \tag{1}$$

where ϵ is the characteristic relaxation time and D/Dt represents the total derivative. τ^*_{ij} is the Newtonian equilibrium shear stress:

$$\tau^*_{ij} = 2\mu(e_{ij} - \Delta\delta_{ij}/3) \tag{2}$$

where μ is the coefficient of viscosity and:

$$e_{ij} = \frac{1}{2}\left(\frac{\partial u_i}{\partial x_j} + \frac{\partial u_j}{\partial x_i}\right) \tag{3}$$

In Eq. (2), $\Delta = e_{ij}$ and δ_{ij} is the Kronecker delta function, whereas u_i represents the macroscopic velocity in the x_i direction.

It should be emphasized that relaxation equations such as Eq. (1) are not presumed to model the detailed physics involved.[6] They do, however, introduce the dominant effect of interest in a rational way. Subsequently, ϵ may be scaled (to the local molecular collision time) in order to mimic the actual physics. Note that this type of relaxation model (originally attributed to Maxwell) has been applied to conduction phenomena by Chester[7] and may be relevant to mass diffusion processes as well.

Consider the steady, two-dimensional viscous flow adjacent to a solid boundary in a uniform freestream. The governing equations of continuity and momentum are:

$$\frac{\partial u}{\partial x} + \frac{\partial v}{\partial y} = 0 \tag{4}$$

and:

$$u\frac{\partial u}{\partial x} + v\frac{\partial u}{\partial y} = \rho^{-1}\frac{\partial \tau}{\partial y} \tag{5}$$

In Eqs. (4) and (5), u and v represent the streamwise and normal components of velocity, corresponding to x and y, respectively. ρ is the (constant) local fluid density and τ the dominant component of τ_{ij}. To close this system of equations, the following form for the shear stress relaxation equation [Eq. (1)] is appropriate:

$$\epsilon\left(u\frac{\partial \tau}{\partial x} + v\frac{\partial \tau}{\partial y}\right) + \tau = \mu\frac{\partial u}{\partial y} \tag{6}$$

The equations of momentum [Eq. (5)] and shear stress [Eq. (6)] may be transformed into a streamwise position/streamfunction coordinate system, resulting in:

$$\frac{\partial u}{\partial x} - \frac{\partial \tau'}{\partial \psi} = 0 \tag{7}$$

and:

$$\epsilon\frac{\partial \tau'}{\partial x} - \nu\frac{\partial u}{\partial \psi} = -\tau'/u \tag{8}$$

where $\nu \equiv \mu/\rho$, $\tau' \equiv \tau/\rho$ and ψ ($\partial\psi/\partial y \equiv u$ and $\partial\psi/\partial x \equiv -v$) is established by satisfying the continuity equation. Equations (7) and (8) have real characteristics defined by:

$$\frac{d\psi}{dx} = \pm(\nu/\epsilon)^{1/2} \tag{9}$$

along which:

$$\epsilon d\tau' \pm (\epsilon\nu)^{1/2} du = -(\tau'/u)dx \tag{10}$$

Therefore, the influence of zero shear stress and uniform velocity properties, typically associated with the external flow initial conditions, propagates along characteristics for all nonzero ϵ. The solution of the equations in this case does not result in an asymptotic approach to freestream conditions yet continuously approaches the parabolic solution as $\epsilon \to 0$, which may be utilized as a convenient artifice for numerical computation.

Apart from explaining analytical solution anomalies associated with the use of diffusive transport models, it is of interest to determine under what circumstances *measurable* nonequilibrium phenomena may be encountered. If the conditions which support nonequilibrium transport are achievable in experimental or flight conditions, equilibrium engineering models of the associated flowfields will be inherently approximate and might conceivably result in analytical predictions that are of less than acceptable accuracy.

For the flowfield studied here, Eq. (8) may be evaluated as an external streamline penetrates the boundary-layer, where nonequilibrium effects would be most readily observed. Consider the case of a constant velocity fluid "particle" that instantaneously enters a region of uniform velocity gradient. Nondimensionalizing Eq. (8) by the characteristic length (L) and equilibrium Newtonian shear stress ($\nu u \partial u/\partial\psi$) provides the following relationship:

$$\epsilon\left\{\frac{u}{L}\right\}\frac{\partial \tilde{\tau}'}{\partial \tilde{x}} + \tilde{\tau}' = 1 \tag{11}$$

$\tilde{\tau}'$ and $\tilde{x}$ are the resultant dimensionless variables in Eq. (11), which has the following exact solution:

$$\tilde{\tau}' = 1 - \exp(-\tilde{x}/\lambda) \tag{12}$$

where

$$\lambda \equiv \epsilon u/L \tag{13}$$

The e-folding shear stress ($\tau' = 63\%$ of equilibrium) will occur at $\tilde{x} = \lambda$. A *conservative* estimate of the measurable (observable) equilibrium lag is $\tilde{x} = 10^{-3} \to 10^{-2}$, depending on the probe/experimental dimensions or the streamwise computational mesh. Therefore, the regime in which nonequilibrium effects become important may be defined by:

$$\epsilon u/L = 10^{-3} \to 10^{-2} \tag{14}$$

The various conceivable experimental or flight conditions involve characteristic velocities and lengths in the ranges $u = 10^2 \to 10^3$ m/s and $L = 10^{-1} \to 10^2$ m. Therefore, the critical values of ϵ for which nonequilibrium phenomena first become observable are:

$$\epsilon = 10^{-7} \to 10^{-2}\text{s} \tag{15}$$

A more optimistic evaluation of experimental/computational capabilities could reduce the minimum critical ϵ to 10^{-8}. From kinetic theory,[2,3] the equilibration time constant (ϵ) is of the order of several (n) molecular collision times (ℓ/c), which may be written:

$$\ell/c = k(\rho\mu)^{-1} \tag{16}$$

In Eq. (16), ℓ is the molecular mean free path, c the characteristic molecular velocity, and k the proportionality factor in the equation $\rho\ell = (2k)^{1/2}$. Therefore, given that $n = 10^0 \rightarrow 10^1$, the equilibration time, $\epsilon = n\ell/c$ enters the critical range [defined by Eq. (15)] in the standard atmosphere at an elevation of 3×10^4m, or in corresponding experimental conditions. Subsequent reductions in density further increase the observable nonequilibrium effects.

In a different transport modeling context, application of the relaxation equation to turbulent flows also has intuitive appeal, inasmuch as the elements of the Reynolds stress tensor are governed by convective equations. In this case, the formulation utilized here closely resembles currently evolving transport theories, such as the one developed by Bradshaw,[8] which also result in a hyperbolic system of equations.

This particular turbulence modeling approach does not require support from the physics of higher order kinetic theory. However, their resultant similar mathematical nature brings some unity to the consequences of adopting a particular class of transport model. Quite often, the modeling of physical processes leads naturally to a hyperbolic system of governing equations.[9] It is then desirable to expose the physical source of the limiting (often parabolic) mathematical nature of commonly used approximate transport models. Subsequently, it is not nearly so surprising when rigorous hyperbolic models are resurrected for particular applications.

References

[1] Batchelor, G.K., *An Introduction to Fluid Dynamics,* Cambridge University Press, 1970.

[2] Jeans, J.H., *The Dynamical Theory of Gases,* Cambridge University Press, 1925.

[3] Chapman, S. and Cowling, T.G., *The Mathematical Theory of Non-Uniform Gases,* Cambridge University Press, 1952.

[4] Onsager, L., *Physical Review,* Vol. 37, Feb. 15, 1931, p. 405; Vol. 38, Dec. 15, 1931, p. 2265.

[5] Lighthill, M.J., "Viscosity Effects In Sound Waves of Finite Amplitude," *Surveys In Mechanics,* edited by G.K. Batchelor and R.M. Davies, Cambridge University Press, 1956.

[6] Grad, H., "The Kinetic Theory of Rarefied Gases," *Communications on Pure and Applied Mathematics,* Vol. 2, Dec. 1949, pp. 331-407.

[7] Chester, M., "Second Sounds in Solids," *Physical Review.,* Vol. 131, Sept. 1963, pp. 2013-2015.

[8] Bradshaw, P., Ferris, D.H., and Atwell, N.P., "Calculation of Boundary Layer Development Using the Turbulent Energy Equation," *Journal of Fluid Mechanics,* Vol. 28, May 26, 1967, pp. 593-616.

[9] Whitham, G.B., *Linear and Nonlinear Waves,* Wiley-Interscience, New York, 1974.

Criteria for Asymptotic Supersonic Two-Dimensional Turbulent Wakes

Michael J. Walsh*

NASA Langley Research Center, Hampton, Va.

Nomenclature

C_D = body drag coefficient, $\frac{2}{H}\int_{y=-\infty}^{\infty} \frac{\rho u}{\rho_\infty u_\infty}(u_\infty - u)\,dy$

H = base height of wedge

L = transverse length scale

Re_H = Reynolds number based on base height of the wedge

T = static temperature

u = longitudinal velocity

$\tilde{u}$ = similarity variable for velocity, $(u_\infty - u)/(u_\infty - u_0)$

x = longitudinal distance downstream of the wedge

y = transverse coordinate

$y_{1/2}$ = wake half-width

η = similarity variable for y coordinate, y/L

θ = temperature defect, $(T_0 - T_\infty)/T_\infty$

ρ = gas density

ω = velocity defect, $(u_\infty - u_0)/u_\infty$

Subscripts

e = edge of viscous wake

∞ = freestream

0 = centerline

T = quantity determined from temperature profiles

Superscript

$*$ = physical variable transformed to Howarth-Doroditzen coordinates

Received Oct. 6, 1978; revision received Feb. 20, 1979. This paper is declared a work of the U.S. Government and therefore is in the public domain.

Index categories: Jets, Wakes, and Viscid-Inviscid Flow Interactions; Supersonic and Hypersonic Flow.

*Aerospace Engineer, Fluid Mechanics Branch, High-Speed Aerodynamics Division. Member AIAA.

SEVERAL sets of experimental data exist to validate turbulence models for two-dimensional supersonic turbulent wakes.[1-7] To use these data for turbulence modeling requires determination of the extent of the fully developed turbulent region. Birch and Eggers[8] note that for a turbulent flow to be fully developed, the mean as well as the turbulence components must be similar and an asymptotic growth rate attained. In the past, the location of the fully developed turbulent flow in two-dimensional supersonic wakes has not been that well defined. References 4, 6, and 7 used similarity variables of the mean flow, while Ref. 3 examined the wake growth rates. Demetriades[7] found that the velocity profiles were not similar until the flow was fully developed turbulent; however, Wagner[4] found that his profiles were similar a considerable distance upstream of the point where he would expect the mean turbulent wake flow to be fully developed.

The purpose of this Note is to examine the similarity variables that have been used in the past to determine fully developed mean flow for supersonic two-dimensional wakes and to demonstrate that wake growth rates are better indicators that the mean flow is fully developed.

Demetriades[6] used the following similarity variables:

$$\tilde{u} = (u_\infty - u)/(u_\infty - u_0) \tag{1}$$

and

$$\eta = y^*/L \tag{2}$$

where the transverse length scale is related to the body drag coefficient C_D as follows

$$L = C_D H/4\omega \tag{3}$$

The variable H is the base height of the wedge, ω is the velocity defect, and u_∞ and u_0 are the freestream and centerline velocities, respectively. The variable y^* is the physical y distance transformed to Howarth-Dorodnitzen coordinates using the following equation:

$$y^* = \int_0^y \frac{\rho}{\rho_\infty}\,dy \tag{4}$$

Because he used a slender wake generator, Demetriades[6] was able to neglect the recompression and expansion waves present in a supersonic wake and assume that the properties at